Compositional Zoning and Its Significance in Pyroxenes from Three Coarse-Grained Lunar Samples

Abstract. *The calcium-rich pyroxenes in lunar samples 10047, 10058, and 10062 show pronounced sectoral and radial compositional variations which correlate with sharp to gradual variations in color and optical properties. The pyroxenes apparently grew as nearly euhedral crystals from melts of approximately the same composition as that of the samples. The coupled substitutions determined across sector boundaries suggest that Al is predominantly in the tetrahedral site and that Ti is predominantly quadrivalent. The pyroxene differentiation trend (unknown in terrestrial pyroxenes) is toward extreme enrichment in the ferrosilite molecule. The iron-enriched portions of the pyroxene grains may have grown with a triclinic pyroxenoid structure.*

The three type B lunar samples studied (10047, 10058, and 10062) are all ilmenite-rich gabbros with conspicuous reddish brown pyroxene. Sample 47 [54 percent, by volume, pyroxene (Px), 0.7 mm median grain diameter; 27 percent plagioclase (Pc), 0.2 mm; 15 percent ilmenite (Ilm), 0.3 mm; and 4 percent cristobalite (Cr), 0.4 mm] is very similar modally and in grain size to sample 58 (55 percent Px, 0.4 mm; 24 percent Pc, 0.2 mm; 15 percent Ilm, 0.3 mm; 6 percent Cr, 0.3 mm). Sample 62 is much finer grained and contains olivine (Ol) instead of cristobalite (50 percent Px, 0.15 mm; 26 percent Pc, 0.1 mm; 20 percent Ilm, 0.1 mm; 4 percent Ol, 0.25 mm). Sulfide, containing rounded blebs of native iron, is a minor accessory in all three samples; grains of ulvospinel were identified in sample 58, and chromite (in the olivine and ilmenite) and rutile (in the ilmenite) in sample 62. An unidentified Zr mineral, with essential Fe, Ti, Si, and Ca, and significant Y, was also found in sample 58.

The pyroxenes are typically pink, subhedral, and in ophitic or subophitic intergrowth with plagioclase. Prismatic cleavage is rare; the irregular, roughly parallel fractures present represent, in some grains at least, the (001) parting. Zoning is conspicuous in all pyroxenes, manifest in plane polarized light by a sharp to gradual change in color from pink to near colorless. Discontinuous peripheral zones on some grains in sample 47 are distinctly honey-yellow; similar material may also be present, in lesser amount, in sample 58 (Fig. 1, zone *T*). The zoning is emphasized under crossed polarizers, with both sharp and gradual extinction changes coinciding with the plane-light color boundaries. The zone distribution approximates an hourglass pattern in some grains, but in others it appears exceedingly complex, with irregular variations and repetitions. The possibility of occurrence of strain shadows cannot entirely be excluded. The pyroxenes in sample 62 are particularly fractured, with highly irregular extinction patterns; single pyroxene "areas" appear to be composed of a number of separate zoned individuals. Compositional irregularities in probe traverses of these pyroxenes suggest the presence of submicroscopic Ca-poor pyroxene exsolution lamellae.

Optical properties, understandably, show considerable variation. Although those of sample 58 have been studied most intensively, there is considerable overlap between the samples. $2V_z$ measurements on sample 58 vary from 40.5° to 47.5°; $Z \wedge c$ could not be determined precisely but apparently varies more continuously than does 2V. Refractive indices on 13 grains range from Ny = 1.702 to Ny = 1.742, birefringence 0.23 to 0.33. Yellow border phase of sample 47 has $2V_z = 35°$, Ny = 1.750 to 1.755. Efforts to obtain "average" unit cell parameters for the pyroxene in sample 58 resulted in unrealistic values with prohibitively large errors after least-squares refinement. Because of the prevalent zoning, similar attempts on the pyroxene in other samples were abandoned. X-ray powder photographs of the yellow "pyroxene" border phase (handpicked) in sample 47 show it to be significantly different from the pink pyroxene core, suggesting a different (and possibly lower) symmetry for this yellow phase. Qualitatively, the yellow border phase of sample 47 appears equivalent in composition to the outermost zone in sample 58 (Fig. 1, zone *T*).

The compositional variations along microprobe traverses *a* and *b* of one sample 58 pyroxene (Fig. 1) are qualitatively illustrated in Fig. 2. Discontinuities in composition occur at points *B, C,* and *D* (Fig. 2a), and these discontinuities correlate exactly with the extinction discontinuities at *B, C,* and *D* of Fig. 1. Points *A* and *E* of Fig. 2 mark the position of the two outermost extinction discontinuities in Fig. 1, but do not coincide with sharp chemical changes. The composition, best represented by the Fe, Mg, and Ca profiles, varies continuously from points *B* and *D* toward the edges of the crystal, and, with the exception of the slight discontinuity at *C*, is nearly constant between points *B* and *D*. The area of continuous change of composition correlates with a continuous change of extinction angle; conversely, along the line between *B* and *D* no change of extinction angle was observed. Figure 2b shows a second profile, nearly perpendicular to the first

Table 1. Results of eight analyses of pyroxene.

Substance	1	2	3	4	5	6	7	8
				Oxides				
MgO	2.29	16.71	15.13	15.28	16.57	15.39	1.85	14.60
Al_2O_3	0.86	1.58	3.06	2.84	1.66	1.22	0.78	2.78
SiO_2	47.09	51.56	49.40	49.85	51.36	50.78	46.53	49.76
CaO	8.04	15.81	18.66	17.89	16.08	14.53	7.16	20.78
TiO_2	0.72	1.54	2.61	2.54	1.74	1.22	0.78	2.92
Cr_2O_3	.06	0.18	0.28	0.20	0.15	0.10	.04	0.28
MnO	.67	.24	.19	.22	.26	.32	.61	.21
FeO	41.07	12.76	10.45	10.88	13.27	16.56	43.42	9.86
Total	100.8	100.4	99.8	99.7	101.1	100.1	101.2	101.2
				Cation proportions				
Si	1.96	1.92	1.85	1.87	1.91	1.92	1.95	1.85
Al	0.04	0.07	0.14	0.13	0.07	0.06	0.04	0.12
Ti	.02	.04	.07	.07	.05	.04	.03	.08
Cr	.002	.005	.008	.006	.004	.003	.001	.008
Mn	.02	.01	.01	.01	.01	.01	.02	.01
Mg	.14	.93	.85	.85	.92	.87	.12	.81
Fe	1.43	.40	.33	.34	.41	.53	1.52	.31
Ca	0.36	.63	.75	.72	.64	.59	0.32	.83

traverse (Fig. 1, right) and extending from the center of the crystal to the edge. Again, pronounced continuous compositional zoning correlates with a continuous change of the extinction angle.

Table 1 shows total analyses for the points indicated in Fig. 2; the analyses are based on the correction factors of Bence and Albee (*1*), relative to almandine garnet (Fe), synthetic diopside (Ca, Mg, Si), jadeite (Al), ilmenite (Ti), chrome metal (Cr), and spessartine garnet (Mn). Wavelength profiles did not indicate the presence of more than 0.03 percent by weight of any other element. The analyses total close to 100 percent; but the estimated errors are about 2 percent of the amount of the major elements present and about 5 percent for the minor elements, with the exception of Al which may be low by 10 to 20 percent. The formulas shown in Table 1, calculated on the basis of six oxygen atoms to the unit cell, clearly indicate tetrahedral substitution of Al for Si. The substitution of Ti in the M sites, in an amount which is approximately half of the Al substitution of Si, indicates the coupled substitution (Ti + 2 Al) for (2 Si + 1 divalent cation). This coupled substitution implies that the titanium is predominantly quadrivalent. The large possible error in the Al determination arises from the fact that the Al standard (jadeite) has Al in sixfold rather than fourfold coordination. Because the spectrometer was peaked on the jadeite, the correction would increase the atomic proportion of Al to a number closer to twice the titanium content.

The hourglass pattern of areas with coherent optical extinction (Fig. 1) and the discontinuous changes of composition between such areas suggest that the pyroxenes of lunar sample 10058 are sector-zoned. The sector-zoning phenomenon has been described elsewhere in detail for staurolite (*2*) and has been observed (*3*) in titaniferous augite. The profiles of Fig. 2 are remarkably similar in geometric form to those reported for sector-zoned staurolite (*2*). The analyses between the edges and points *B* and *D* (Fig. 2) are within the (110) sectors, and those between *B* and *D* may be within the (001) sector. The small discontinuity at *C* implies another sector, besides the (001) sector, between points *B* and *D*. A number of different sectors are possible in the lunar pyroxenes because pyroxene

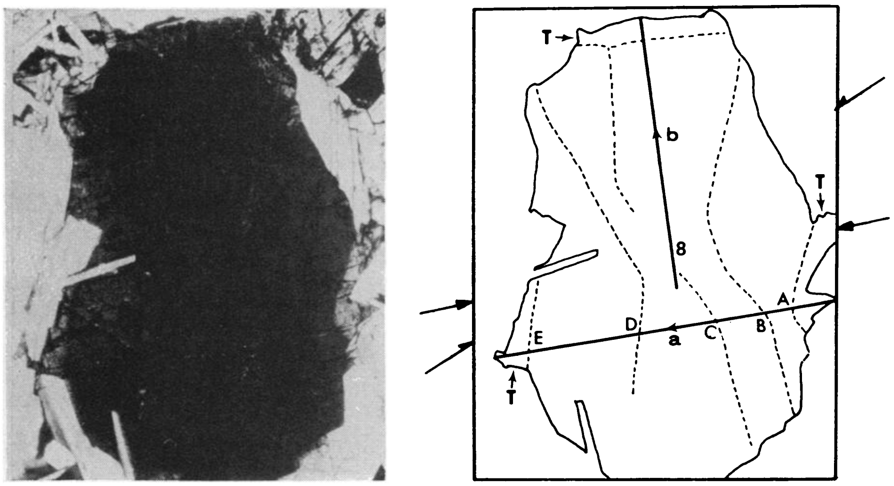

Fig. 1. (Left) Pyroxene crystal from sample 10058; crossed polarizers. (Right) Outline of the crystal at left, showing zone boundaries (broken lines). Heavy lines locate microprobe traverses *a* and *b* (traverse *a* is approximately 1 mm long). Letters *A* through *E* mark positions of discontinuous change of extinction angle. Double-headed arrows parallel (001) parting; single-headed arrows parallel trace of optic axial plane. Zones designated *T* are referred to in text.

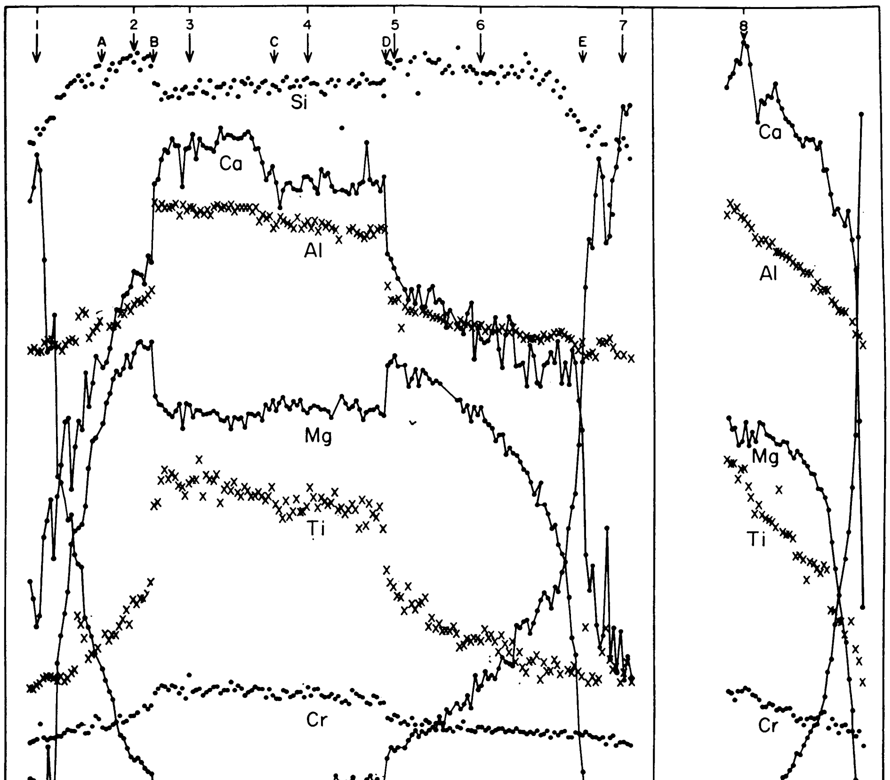

Fig. 2. (a) Variations of the elements Ca, Mg, Fe, Mn, Ti, Cr, Al, and Si along traverse *a* of Fig. 1. (b) Variations of the elements Ca, Mg, Fe, Ti, Cr, and Al along traverse *b* of Fig. 1; point 8 is at the center of the crystal. The letters *A* through *E* mark positions of discontinuous changes of extinction angle. The numbers 1 through 8 mark the horizons where the analyses in Table 1 were determined. Electron beam diameter is less than 1 μ; analysis interval (a) is 6 μ; (b) is 20 μ. Vertical scale (not shown) is counting rate.

typically grows with more than two forms.

The nearly constant composition between *B* and *D* and the continuous change of composition to the edges from *B* and *D* and within the (001) sector (Fig. 2b) are consistent with the sector-zoning interpretation. The constant composition section of the profile is nearly parallel to the (001) crystal face (Fig. 1), which would imply that that part of the profile was parallel to a growth surface which could be expected to have a constant composition; on the other hand, the other profiles are oblique to the growth surfaces and therefore would show any continuous changes of composition with growth.

The major chemical difference between sectors, higher Ti and Al and lower Si in the (001) sector relative to the (110) sectors, is also consistent with the sector-zoning interpretation: On a growing (001) face the M and T sites are exposed simultaneously, whereas on a growing (110) face either an M site or a T site is exposed. The simultaneous exposure of the two sites on (001) facilitates a coupled substitution because a local charge balance can be achieved, whereas a coupled substitution on the (110) face requires a local charge imbalance during the time between additions of growth layers. This type of mechanism is discussed elsewhere for staurolite (*4*). A mechanism to explain the discontinuity of Ca between sectors is not immediately obvious. The sector-zoning model implies, of course, that the lunar pyroxenes were nearly euhedral during most of their growth.

Seven other profiles exhibiting chemical features similar to those of Fig. 2 were made on the pyroxene grain of Fig. 1 and other pyroxene grains in sample 10058. However, they did not all exhibit sharp discontinuities in all elements. Several showed sharp discontinuities of the multivalent cations Ti, Si, and Al, but were diffuse in Fe, Mg, and Ca. It is here suggested that there were originally sharp discontinuities in all the elements but that during the time since the pyroxenes crystallized localized diffusion led to local obliteration of the sharp discontinuities. At some places, the diffusion was only by the divalent cations, but at others all the cations may have been involved. A localized diffusion pattern could lead to a very irregular optical appearance of the pyroxenes.

The very pronounced continuous zoning of Fe, Mg, and Ca (Fig. 2) was noted in pyroxene grains in all three samples. This type of zoning pattern has been reported for garnet (*5*) and suggests that the pyroxenes, as they grew, depleted the matrix (melt) in Mg relative to Fe. The pronounced zoning suggests that the composition of the reservoir from which the pyroxenes grew was the same as that of the rock in which they now occur. This interpretation precludes the possibility of differentiation by physical separation of pyroxene from a large magma chamber. The edge content of Mg in the pyroxene of sample 58 was calculated on the basis of the Rayleigh fractionation model (*5*), and compares favorably to the measured edge content.

The essential characteristic of the compositional variation in these lunar pyroxenes is one of extreme enrichment in the ferrosilite molecule. Analyses 1 and 7 (Table 1), representing the outermost, iron-enriched zones, plot in an area of the pyroxene quadrilateral in which there are no terrestrial equivalents (*6*) and where the stable existence of a single pyroxene phase at low pressures is "forbidden," according to the recent experimental work of Lindsley and Munoz (*7*). These analyses are, nevertheless, almost identical with the most ferrosilite-rich metasilicate phases obtained by Bowen *et al.* (*8*) in the system $CaO–FeO–SiO_2$: 80 $FeSiO_3$, 20 $CaSiO_3$ in monoclinic hedenbergite solid solutions stable below 980°C; and 76 $FeSiO_3$, 24 $CaSiO_3$ in triclinic β-wollastonite solid solutions stable above that temperature. Lindsley and Munoz (*7*), however, found that the maximum amount of ferrosilite that could occur in stable solid solution with either hedenbergite or wollastonite is closer to 60 percent. They attribute the discrepant experimental results of Bowen *et al.* (*8*) to either incomplete reaction or metastable equilibrium. Optically, the yellow border phase of sample 47 pyroxene appears homogeneous; reconnaissance probe study shows that it is similar to the border phase in sample 58, represented by analyses 1 and 7 (Table 1). The x-ray powder pattern of the border phase, however, is distinct from that of the core pyroxene, and, although not yet positively determined, it may represent a triclinic pyroxenoid modification. The closest natural occurrence of this phase is the Skaergaard ferrohedenbergite, deemed to have inverted from the ferriferous β-wollastonite form (*9*). This inversion rendered original single crystals into a mosaic of smaller clinopyroxene grains with slightly different orientation. A similar process may be responsible for the unusual complex patchwork texture of the pyroxenes in sample 62, although the possibility of shock deformation cannot be excluded.

If a ferriferous calcium metasilicate with pyroxenoid structure is indeed present, whether or not it is a metastable phase (*7*), then probably the solidus for these rocks was above 980°C (*8*, p. 213). The 1933 prediction of Bowen *et al.* (*8*, p. 270) "that somewhere wollastonites with relatively high amounts of $FeSiO_3$ should be found" will have been surprisingly fulfilled.

R. B. HARGRAVES
L. S. HOLLISTER
G. OTALORA

Department of Geological and Geophysical Sciences, Princeton University, Princeton, New Jersey

References and Notes

1. A. Bence and A. Albee, *J. Geol.* **76**, 382 (1968).
2. L. Hollister and A. Bence, *Science* **158**, 1053 (1967).
3. J. Preston, *Amer. Mineralogist* **51**, 1227 (1966); A. L. Smith and I. S. E. Carmichael, *ibid.* **54**, 909 (1969).
4. L. Hollister, *ibid.*, in press.
5. ———, *Science* **154**, 1647 (1966).
6. W. A. Deer, R. A. Howie, J. Zussman, *Rock Forming Minerals* (Wiley, New York, 1963), p. 5.
7. D. H. Lindsley and J. L. Munoz, *Amer. J. Sci.* **267-A**, 295 (1969).
8. N. L. Bowen, J. F. Schairer, E. Posnjak, *ibid.* **26**, 193 (1933).
9. G. M. Brown and E. A. Vincent, *J. Petrol.* **4**, 175 (1963).
10. We thank N. Dorety, T. Forseman, C. Kulick, D. Roy, R. Warren, and J. Wolinski (Princeton University) for assistance in preparing the samples for analysis and for assistance in the reduction of the data.

4 January 1970